Methodology for the Study of Dynamic ON-Resistance in High-Voltage GaN Field-Effect Transistors

Donghyun Jin, *Student Member, IEEE*, and Jesús A. del Alamo, *Fellow, IEEE*

***Abstract*— We have developed a new methodology to investigate the dynamic ON-resistance (R_{ON}) of high-voltage GaN field-effect transistors. The new technique allows the study of R_{ON} transients after a switching event over an arbitrary length of time. Using this technique, we have investigated dynamic R_{ON} transients in AlGaN/GaN high-voltage, high electron-mobility transistors over a time span of ten decades under a variety of conditions. We find that right after an OFF-to-ON switching event, R_{ON} can be several times higher under dc conditions. The increase in R_{ON} is enhanced as the drain–source voltage in the OFF-state increases. The R_{ON} recovery process after an OFF-to-ON switching event is characterized by a fast release of trapped charge through a temperature-independent tunneling process followed by conventional thermally activated detrapping on a longer timescale. After a high-power-to-ON switching event, in contrast, detrapping only takes place through a temperature-independent process. We postulate that the fast temperature-independent detrapping originates from interface states at the AlGaN barrier/AlN spacer interface. The thermally activated detrapping can arise from traps at the surface of the device or inside the AlGaN barrier. These findings are relevant in the quest to engineer a reliable GaN power switch with minimum dynamic R_{ON} problems.**

***Index Terms*— Border traps, current collapse, dynamic ON-resistance, FET, GaN, high electron-mobility transistor (HEMT), transient, trapping.**

I. Introduction

IN THE last few years, there has been a tremendous interest in the development of energy-efficient electrical power management systems. Recently GaN field-effect transistors have emerged as a disruptive technology with great potential for improved power switching performance. This arises from the outstanding material properties of GaN [1]. A better than three orders of magnitude improvement in ON-resistance/breakdown-voltage tradeoff is projected to be achievable with GaN FETs over current Si-based power-switching technology [2].

Manuscript received March 30, 2013; revised May 24, 2013 and July 9, 2013; accepted July 14, 2013. Date of publication August 2, 2013; date of current version September 18, 2013. This work was supported in part by U.S. Department of Energy in the context of the Agile Delivery of Electric Power Technology Program under Grant DE-AR0000123, the Semiconductor Research Corporation under Grant 2011-VJ-2162, and the DRIFT MURI under an ONR Grant N00014-08-1-0655. The review of this paper was arranged by Editor G. Meneghesso.

The authors are with the Microsystems Technology Laboratories, Massachusetts Institute of Technology, Cambridge, MA 02139 USA (e-mail: jinnara@mit.edu; alamo@mit.edu).

Color versions of one or more of the figures in this paper are available online at http://ieeexplore.ieee.org.

Digital Object Identifier 10.1109/TED.2013.2274477

Among several technical requirements on an efficient power switch, a critical one is obtaining a very low ON resistance (R_{ON}) immediately after switching from a high-voltage OFF state to a low-voltage ON state. In more mature RF power GaN high electron-mobility transistors (HEMTs), dynamic switching problems, such as current collapse, gate lag, and drain lag, are often present and detract from RF power performance [3], [4]. In power switching applications, these same issues manifest themselves as a dynamic R_{ON} in which after an OFF-ON switching event, R_{ON} remains high for a period of time [5], [6]. To date, there has been little research on this important issue [7], [8].

Toward the goal of achieving fundamental understanding of this problem, we have developed a new dynamic R_{ON} transient measurement methodology which allows the observation of R_{ON} transients after a switching event over a time period that can span many decades. This technique combines the measurements of two different instruments. The acquired dynamic ON-resistance transients are then analyzed using a current-transient methodology recently developed [9].

We demonstrate the usefulness of this approach by carry out a systematic study of dynamic R_{ON} on high-voltage GaN-HEMTs on SiC substrate as a function of time, temperature, and pulse conditions. In the samples that we have investigated, we find that after biasing at an OFF-state voltage, the initial value of R_{ON} increases as the voltage increases. Also, on a short timescale, we find that R_{ON} recovers in a temperature-independent manner. In contrast, on a longer timescale, the R_{ON} transients are found to be thermally activated.

We propose that the fast recovery behavior takes place through an electron-tunneling process from traps located inside the AlGaN barrier close to the GaN channel layer. Likely candidates are interface states at the AlN spacer/AlGaN barrier interface. The slower thermally activated recovery is attributed to traps in the AlGaN or at the surface.

This paper provides a methodology toward understanding and mitigating dynamic R_{ON} issues in high-voltage GaN FETs. This paper presents an augmented version of a recent conference presentation [10]. It is organized as follows. Section II explains the measurement technique. Section III briefly describes the devices used to illustrate the technique and presents detailed results obtained under different conditions. Section IV illustrates the importance of epitaxial growth details on dynamic R_{ON}. Lastly, Section V hypothesizes the physical origin of the trapping behavior that is observed.

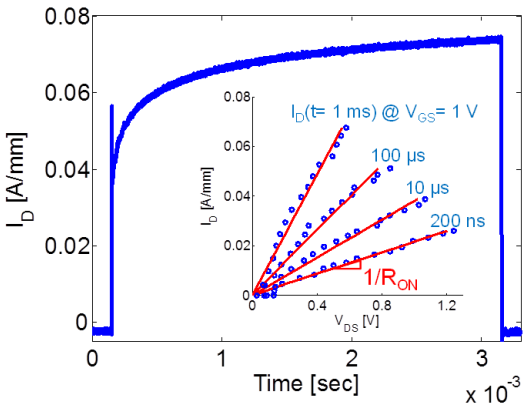

Fig. 1. I_D waveform measured by pulsed I–V system. The device is synchronously switched from an OFF-state quiescent bias of $V_{GSQ} = -10$ V, $V_{DSQ} = 50$ V to an ON-state of $V_{GS} = 1$ V and V_{DS} changing from 50 mV to 1.2 V at ambient temperature of 25 °C. Through the simultaneous measurement of both $I_D(t)$ and $V_{DS}(t)$ transients in the linear regime, the instantaneous R_{ON} (200 ns $\leq t \leq$ 3 ms) is extracted as shown in the inset.

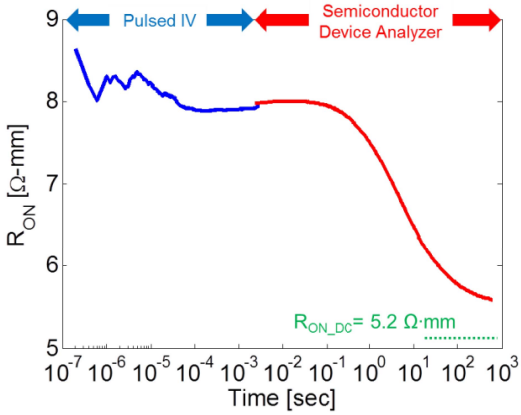

Fig. 2. R_{ON} transients from 200 ns to 1000 s on GaN-on-SiC high-voltage HEMTs from an OFF state ($V_{GSQ} = -5$ V, $V_{DSQ} = 40$ V) to ON-state switching at ambient temperature of 55 °C. Blue line is obtained from pulsed I–V system (Auriga AU4750) and red line from SDA (Agilent B1500A). Also shown are the dc values of R_{ON} obtained after fully detrapping the device (marked as R_{ON_DC}). This shows 66% higher R_{ON} at 200 ns than in dc.

II. Dynamic R_{ON} Measurement Technique

The dynamic R_{ON} measurement technique that we have developed is capable of collecting R_{ON} transients from 200 ns to any arbitrary length of time. For this, we use two different instruments: an Auriga AU4750 pulsed I–V system for R_{ON} transients from 200 ns to 3 ms and an Agilent B1500A semiconductor device analyzer (SDA) for R_{ON} transients beyond 3 ms. In both the cases, synchronous switching of V_{GS} and V_{DS} is performed.

With the pulsed I–V system, we successively switch from an OFF-state quiescent (Q) bias to an ON state given by $V_{GS} = 1$ V and several V_{DS} values in the linear regime of device operation ($\leq$1.2 V). In this manner, we measure the linear drain current characteristics close to the origin. Fig. 1 shows a typical measured I_D waveform in a high-voltage GaN HEMT after it is switched from an OFF state ($V_{GSQ} = -10$ V, $V_{DSQ} = 50$ V) to ON state. $I_D(t)$ and $V_{DS}(t)$ are measured every 200 ns within a pulse width of 3 ms and a duty cycle of 10%. For each data point, the measurement time is 5 ns. To minimize noise and enhance measurement accuracy, each extracted data point represents an average of 300 measurements. As a result of heavy electron trapping that occurs during the OFF-state period, ON-state I_D in the linear regime shows a very slow increase in time toward the expected dc value. In addition, because the pulsed I–V system itself has an internal source resistance, as the device R_{ON} decreases, the range of V_{DS} values in the ON state decreases accordingly. Through the simultaneous measurement of both $I_D(t)$ and $V_{DS}(t)$ transients in the linear regime (Fig. 1, inset), the instantaneous R_{ON} (200 ns $\leq t \leq$ 3 ms) can be extracted.

R_{ON} transients for longer time periods can be explored using SDA. The synchronous pulsed mode of B1500A allows the continuous measurement of R_{ON} transient from 3 ms to any arbitrary time. In contrast to the pulsed I–V system, B1500A can measure $I_D(t)$ transients at a constant V_{DS} value (0.5 V has been used here). By adjusting the time that the device resides in the OFF state, one can closely match the beginning of transient as measured by SDA with the end point of the transient measurement obtained by the pulsed I–V system and obtain a complete transient that spans many decades of time. One example is shown in Fig. 2 for the transients obtained over ten decades. The blue line is measured from the pulsed I–V system and the red one comes from SDA. Also shown are the DC values of R_{ON} obtained after fully detrapping the device under visible light illumination.

In these synchronous pulsed measurements using the pulsed I–V system and SDA, fast switching of V_{GS} and V_{DS} is important so as to prevent the occurrence of a momentary high-power state during the transition (hard switching). Fig. 3 shows the waveforms of three different switching events from the OFF state ($V_{GSQ} = -5$ V, $V_{DSQ} = 40$ V) to the ON state in one of the test samples. These measurements are obtained through the pulsed I–V system. In one event, the pulsing of V_{DS} and V_{GS} is synchronous. In the other two events, a delay of 200 or 400 ns is introduced between the switching-off of V_{DS} and the switching-on of V_{GS}. The corresponding R_{ON} transient measurements are shown as follows.

The time lapse between the samples in the waveforms at the top of Fig. 3 is 5 ns. With our relatively small-size devices, when tested through the pulsed I–V system, a fast slew late of 1 V/ns is measured. In the synchronous case, this results in a very short overlap (a few nanoseconds) of V_{DS} and V_{GS} waveforms at relatively low values of V_{DS}. This does not introduce any visible trapping in the device as evidenced by the resulting R_{ON} transients which are essentially identical to those obtained when a delay of 200 or 400 ns is introduced between the two pulses. The situation might be different in the case of large-size devices where the slew rate can be significantly slower and an adjustment of delay time between V_{DS} and V_{GS} pulses might be needed.

In the synchronous pulse mode of B1500A, there is no way to control the relative delay between the gate and drain pulses. However, because the switching occurs on a much slower time scale and we always observe a good match of characteristics at the boundary with the data acquired from the pulsed I–V

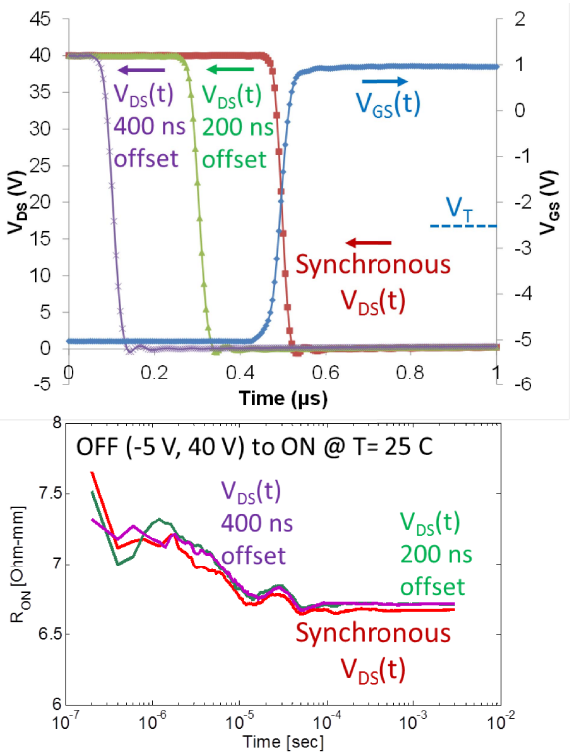

Fig. 3. Top: V_{DS} and V_{GS} waveforms of three switching events from an OFF state ($V_{GSQ} = -5$ V, $V_{DSQ} = 40$ V) to ON state. In one event, the pulsing is synchronous. In the other two, a delay of 200 ns or 400 ns is introduced between the falling edge of V_{DS} and the rising edge of V_{GS}. Bottom: resulting R_{ON} transients are unaffected by the relative alignment of V_{DS} and V_{GS} pulses, indicating that trapping during the transient is negligible. In our relatively small size devices, a fast slew late of 1 V/ns is obtained.

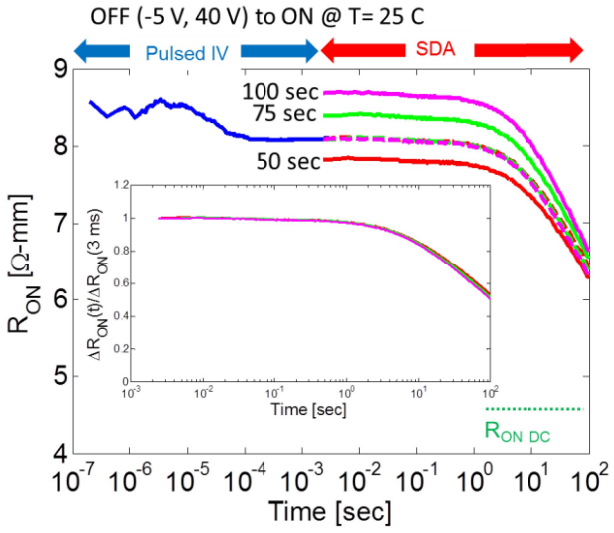

Fig. 4. R_{ON} transients in OFF ($V_{GSQ} = -5$ V, $V_{DSQ} = 40$ V) to ON-state switching from pulsed IV in the blue line and from SDA using different OFF-state times of 50, 75, or 100 s. A visible mismatch occurs with the pulsed IV data. Scaling the SDA-obtained data to match $\Delta R_{ON}(t)/\Delta R_{ON}$ (3 ms) makes all lines overlap with each other as shown in dotted line. Inset: identical normalized R_{ON} recovery rates suggesting that the R_{ON} transients are largely independent of the initial value of R_{ON} (3 ms).

system, we conclude that any hard switching that might occur results in negligible trapping on the time scale in which we use this tool ($t > 3$ ms).

The stitching approach shown in Fig. 2 is time-consuming and inevitably leaves a small residual discrepancy between the measurements obtained through the two techniques at 3 ms stitching point. This can cause noise in the final time constant spectra [9]. We have eliminated this problem by appropriately scaling the transient data obtained from SDA. Fig. 4 shows how this scaling works. We show here R_{ON} transients obtained with the pulsed I–V system, as specified earlier, and SDA. Both sets of transients are obtained with the device at the same OFF-state bias point. Before SDA measurements, the device is kept in the OFF state for 50, 75, or 100 s. All of them result in a visible mismatch with the pulsed IV data. As the OFF-state time increases, the initial value of R_{ON} at 3 ms increases because of higher electron trapping. The evolution of transient beyond that initial point, however, is independent of this initial value. This can be seen in the inset of Fig. 4 that graphs $[R_{ON}(t) - R_{ON\_DC}]/[R_{ON}(t = 3\ \text{ms}) - R_{ON\_DC}]$ for the three cases. As seen, the transients closely overlap each other. This suggests that the R_{ON} transients are largely independent of the initial value of R_{ON} at 3 ms and that simple scaling can be used to stitch the R_{ON} measurements obtained from SDA to those derived from pulsed I–V system.

From this paper, we have synthesized the following approach to obtain complete R_{ON} transients. First, an R_{ON} transient is obtained using the pulsed I–V system. Then, the OFF-state time in the B1500A is controlled to produce an R_{ON} transient that closely matches the final value obtained from the pulsed I–V system. The residual mismatch is resolved through scaling of B1500A data set to match with the pulsed IV data at $t = 3$ ms. The overall transient is then analyzed using the time constant spectrum approach of [9].

III. Dynamic R_{ON} in High-Voltage GaN HEMTs on SiC

We have demonstrated the usefulness of our proposed dynamic R_{ON} technique by studying in detail industrially prototyped AlGaN/GaN HEMTs grown by metal organic chemical vapor deposition on SiC for S-band power amplifier application. The heterostructure includes a GaN cap and an AlN spacer. The device design features an integrated field plate and a source-connected field plate. The gate width is $6 \times 100\ \mu$m. The devices are depletion mode with a threshold voltage ~ -3 V. The breakdown voltage of devices is ~ 160 V. All the measurements are performed in dark and in air. There was no discernible permanent degradation of devices as a result of repeated testing under the conditions used in this paper.

Fig. 2 shows R_{ON} transients from representative devices when the device is switched from an OFF state with $V_{GSQ} = -5$ V and $V_{DSQ} = 40$ V at $T = 55$ °C. R_{ON} at 200 ns is $\sim$66% higher than in dc (R_{ON_DC}). Such a high dynamic R_{ON} represents a big problem for power-switching applications. The pattern of recovery of R_{ON} exhibits a very slow transient in the s–ks time range.

To gain insight into the physics of this dynamic behavior, we have carried out OFF to ON transients from different quiescent V_{DS} values at ambient temperature, as shown in Fig. 5.

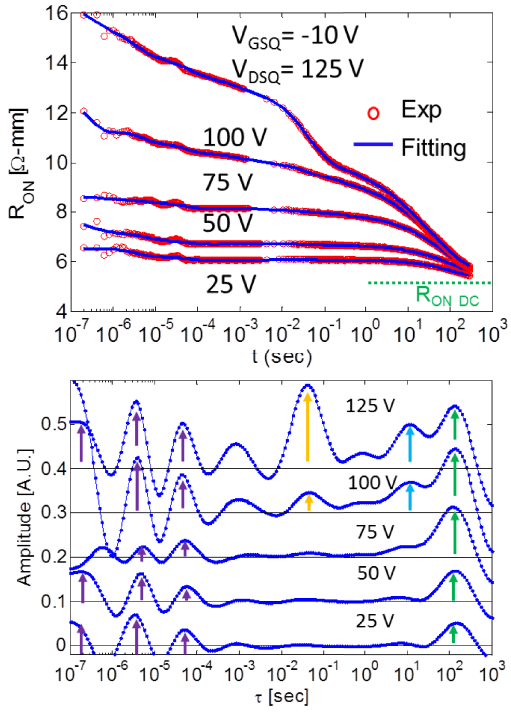

Fig. 5. Top: dynamic R_{ON} transients after OFF-to-ON switching events from different quiescent V_{DS} conditions from V_{DSQ} = 25 V to 125 V in 25 V increments at ambient temperature of 25 °C. Red dots are measurements and blues lines are fitting curves through a sum of exponential terms with time constants ranging from 10^{-7} to 10^{3} s as shown in the bottom. The device exhibits prominent time constants in the 1–1000 s range and some in the submicrosecond to millisecond range. As V_{OFF} increases, the dynamic R_{ON} also increases, but the time constants do not change.

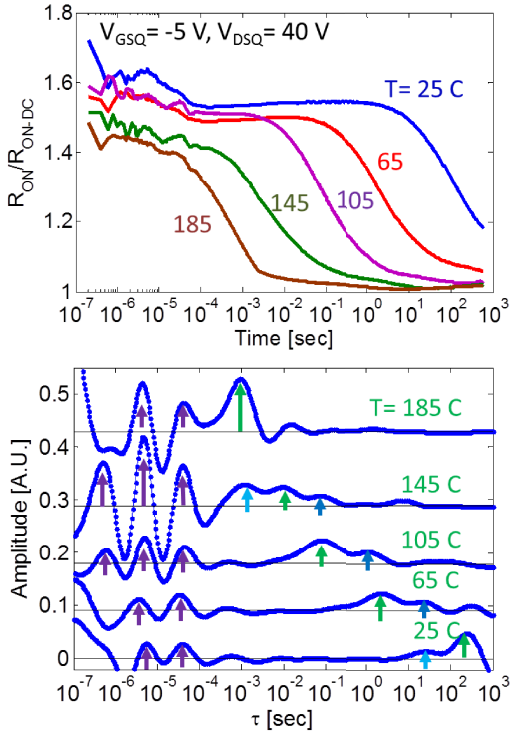

Fig. 6. Top: R_{ON}/R_{ON_DC} transients at different ambient temperatures for $V_{GSQ} = -5$ V and $V_{DSQ} = 40$ V. The resulting time constant spectra (bottom) clearly indicate that the dominant transients for long time substantially speed up as the temperature increases, whereas short time constants are independent of temperature.

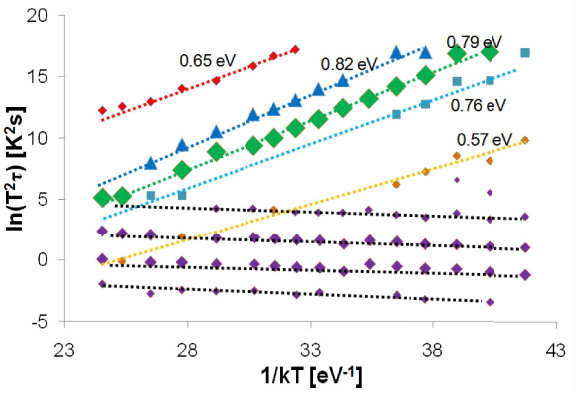

Fig. 7. Arrhenius plot of time constant spectrum of Fig. 6. The size of the symbols is proportional to the height of time constant peak. Dominant traps at 0.79, 0.82, and 0.76 eV are identified. A set of short time constants, which are independent of temperature, are also observed. They are responsible for fast transients.

As V_{DSQ} increases, the dynamic R_{ON} increases in a prominent manner presumably as a result of increased extension of high-field region into the drain.

The dominant time constants underlying these transients can be obtained using a time constant spectrum analysis [9]. We use a sum of exponentials with 20 time constants per decade within the range from 10^{-7} to 10^{3} s. Examples of fits are shown at the top of Fig. 5 and the resulting time constant spectra are shown on the bottom of this figure. These indicate that there are multiple time constants with values that do not change as the applied electric field in the OFF state increases. Only the magnitude of the signals are affected by increasing V_{DSQ}. In particular, there are two prominent time constants in the 10–1000 s range and some more in the submicrosecond to millisecond range. All get more prominent as V_{DSQ} increases. There is also a time constant ~50 ms that prominently increases when V_{DSQ} > 100 V. This could be because of the depletion region sweeping through a particular defect at higher values of V_{DSQ}.

To further understand the physical processes behind these transients, we have performed dynamic R_{ON} measurements at different ambient temperatures and their time constant spectra have been derived as presented in Fig. 6. In this figure, the dominant transients substantially speed up as the temperature increases. The time constant spectra at different temperatures show this acceleration very clearly. Dynamic R_{ON} at 200 ns shows slightly negative dependence as the temperature increases. This is most likely because of the high voltage trapping process resulting in less trapping as the temperature increases because in the OFF state, there is always a counterbalancing detrapping process that is enhanced. In addition to this, the device also exhibits fast transients that change less with temperature. This temperature-independent behavior for short times is also verified in the corresponding spectra.

Following the methodology of [9], we have plotted the evolution of dominant time constants with temperature in an Arrhenius plot (Fig. 7). The size of the symbols in this figure is

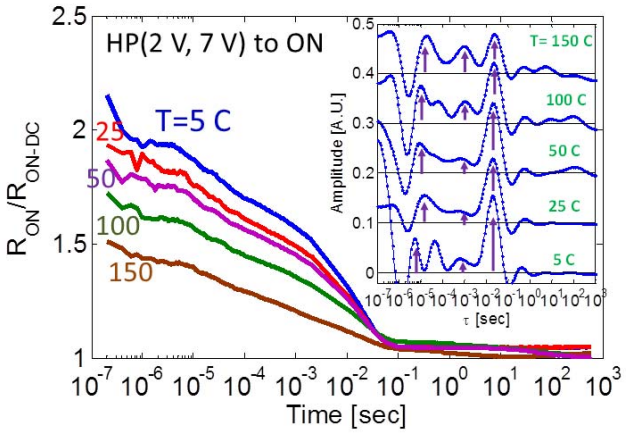

Fig. 8. High power to ON-state transients at different ambient temperatures and the resulting time constant spectra (inset). The high-power-state bias is $V_{GSQ} = 2$ V and $V_{DSQ} = 7$ V (the power level was 5.4 W/mm at ambient temperature of 25 °C corresponding to the red line). The transients are dominated by temperature-independent fast time constants. No thermally activated slow-transients are observed.

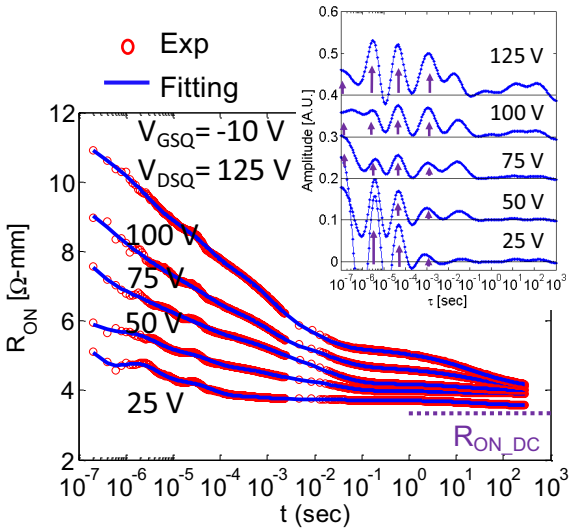

Fig. 9. Dynamic R_{ON} transients in the alternative wafer (see text) after identical OFF-to-ON switching events, as in Fig. 5, at ambient temperature of 25 °C. Inset: corresponding time-constant spectra. In contrast to Fig. 5, devices in this wafer have much weaker time constants in longer time periods, whereas short time constants in the submicrosecond to millisecond range dominate and do not change as V_{OFF} increases.

proportional to the height of the time constant peaks. From this Arrhenius plot, two distinct patterns emerge: a set of long time constants with thermally activated behavior and another set of short time constants that are independent of temperature. The long thermally activated time constants can be associated with conventional traps. The dominant traps are estimated at 0.79, 0.82, and 0.76 eV below the conduction band edge. Traps at similar energies have been reported by other authors in similar structures [11]–[13].

To further clarify the physics, we have also performed high power (HP) to ON transients. Fig. 8 shows the dynamic R_{ON} transients from a quiescent bias of $V_{GS} = 2$ V, $V_{DS} = 7$ V, and their respective time constant spectra at different ambient temperatures. The power level was 5.4 W/mm at ambient temperature of 25 °C corresponding to the red line. The transients are dominated by fast time constants only. In contrast to the data in Figs. 5 and 6, there are no slow thermally activated transients present. Furthermore, the dominant time constants of transients in Fig. 8 are temperature-independent as the spectrum clearly reveals. The initial value of R_{ON}/R_{ON_DC} at 200 ns decreases with temperature, again reflecting a competition between trapping and detrapping during the HP trapping state. These temperature-independent and fast recovery characteristics support the notion that the fast time constant processes that are observed in Figs. 5, 6, and 8 have a common origin. Additional HP-to-ON transients at different V_{DG} values but the same power dissipation [10] reveal that the fast transients emerge from electrons that were trapped through a hot-electron process. Hot-electron phenomena have also been prominently observed in several other studies [12], [14], [15] along with severe impact on R_{ON} degradation.

IV. Impact of Epitaxial Growth on Dynamic R_{ON}

We have studied the importance of epitaxial growth details on dynamic R_{ON} characteristics by applying our methodology to identical devices fabricated on a nominally identical epitaxial wafer that was grown by a different commercial epitaxial vendor. The device layer stack comprising GaN cap, AlGaN barrier, AlN spacer, and GaN channel layer follows an identical design with the same AlGaN mole fraction and thicknesses. Most likely, there are differences in buffer structure design which is the proprietary information of each epitaxy-growth supplier and is unknown to us. This alternative wafer was processed into devices in the same lot with the same layout as the sample discussed earlier in this paper. The breakdown voltage of these new devices is > 200 V.

A different buffer could well result in a different defect structure in the top active layers that produce different dynamic R_{ON} characteristics as evaluated by our methodology. As is the case for the wafer discussed earlier, many different devices have been tested and the results are consistent. The observed differences shown here between devices from the two wafers reflect wafer-to-wafer differences.

Dynamic R_{ON} transients under identical OFF-to-ON switching conditions as in Fig. 5 have been measured in a device from this alternative wafer at ambient temperature of 25 °C and are shown in Fig. 9. The observed pattern of R_{ON} recovery is rather different from those shown earlier. In contrast to the dominance of long time constants in the data of Fig. 5, the alternative wafer exhibits much weaker time constants for longer time periods whereas short time constants in the submicrosecond to millisecond range dominate. This is clearly seen in the time constant spectra shown in the inset of Fig. 9. These measurements show that these two wafers have a rather different defect structure.

Dynamic R_{ON} measurements at different ambient temperatures following trapping at $V_{GSQ} = -5$ V and $V_{DSQ} = 40$ V in the alternative wafer are shown in Fig. 10. These data are equivalent to those of Fig. 6 earlier in this paper. Once again we find that the recovery transients with short time constants

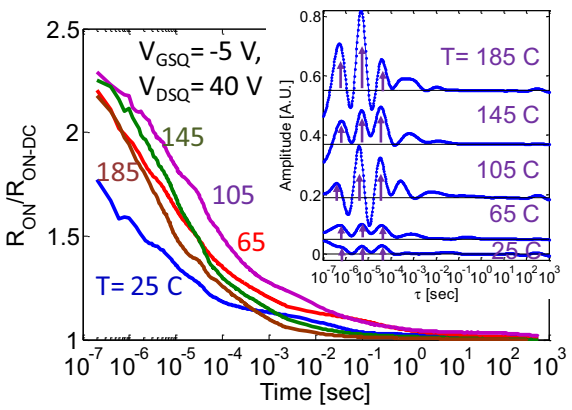

Fig. 10. Top: R_{ON}/R_{ON_DC} transients in devices from the alternative wafer at different ambient temperatures for $V_{GSQ} = -5$ V and $V_{DSQ} = 40$ V. The resulting time constant spectra (inset) show that the dominant transients with short time constants are temperature-independent.

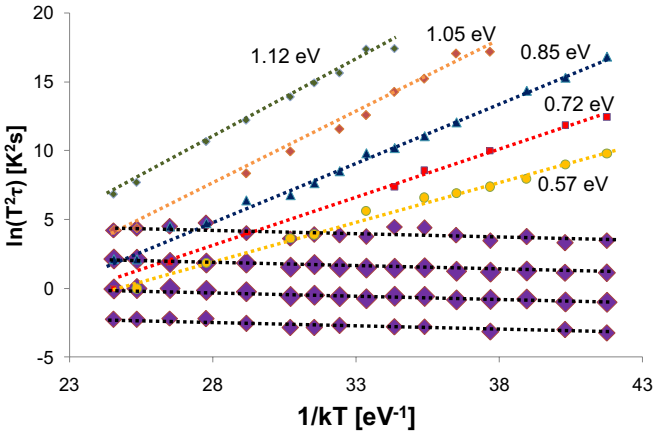

Fig. 11. Arrhenius plot of time constant spectra of Fig. 10. The size of the symbols is proportional to the height of the time constant peak. A rich spectrum of traps with activation energies between 0.57 and 1.12 eV is observed, but their concentration is much lower than that in Fig. 7. The dominant time constants are short and do not exhibit any temperature dependence.

change little with temperature. This temperature- independent behavior is also verified in the corresponding spectra in the inset of Fig. 10.

An Arrhenius plot for the dominant time constants of Fig. 10 is shown in Fig. 11. As shown in Fig. 7, the size of the symbols indicates the magnitude of corresponding time constant. In this alternative wafer, a richer spectrum of traps with energies between 0.57 and 1.12 eV is observed but their concentration is much lower than in Fig. 7. The short time constants are clearly dominant in this wafer and they are again temperature-independent.

These results reveal that there are at least two distinct mechanisms that dominate dynamic R_{ON} transients at short times and at long times. The long time transients are associated with conventional traps. The noticeable differences in the two wafers indicate that these can be engineered through proper growth protocols. The short time transients arise from a different mechanism and both the wafers suffer from it. This suggests that they might be associated with an intrinsic aspect of heterostructure.

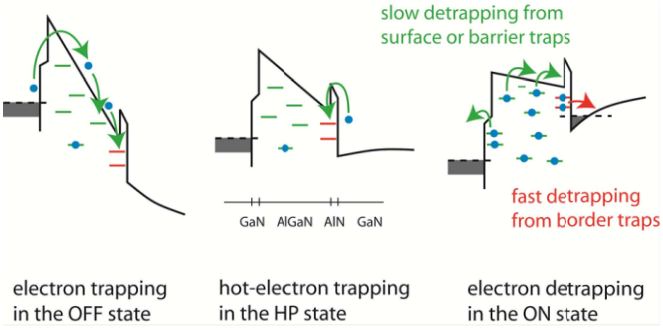

Fig. 12. Postulated mechanisms responsible for dynamic R_{ON} of GaN HEMTs observed in this paper. In the OFF state, electron-trapping at the surface, in AlGaN and at AlGaN/AlN interface, takes place as the electrons flow outside the gate. In the HP state, hot electrons from the channel are trapped at AlGaN/AlN interface states. In the ON state, electron-detrapping takes place thermally for traps in the AlGaN or at the surface and through a tunneling process for AlGaN/AlN interface traps (border traps).

V. Mechanisms Responsible for Dynamic R_{ON}

Our methodology when applied to GaN HEMTs on SiC reveals a rich dynamic behavior of R_{ON}. A picture that can explain all the experimental observations described earlier is shown in Fig. 12. In the OFF state, electrons are trapped as they flow outside the gate into the AlGaN barrier and eventually into the channel (Fig. 12, left). These electrons can be trapped inside AlGaN, at the surface or at the interface states at the AlGaN/AlN interface right above the channel [16]. In the HP state, on the other hand, electrons in the channel gain kinetic energy and overcome the energy barrier with the AlGaN and get trapped. possible sites for this trapping process are interface states at the AlGaN/AlN interface right above the channel (Fig. 12, middle).

During the detrapping process that follows OFF state biasing, we observe fast temperature-independent detrapping processes as well as long thermally activated detrapping processes. On the other hand, after HP-state trapping, only fast temperature-independent detrapping is observed. This suggests that the fast processes observed in both the cases have the same origin and that detrapping takes place through a tunneling process. This is consistent with detrapping from interface states at the AlGaN/AlN spacer interface [16], [17]. Traps that are physically located behind a barrier, but very close to the channel and that release their electrons through a tunneling process, are known as border traps [18]. We postulate that AlGaN/AlN interface states behave as border traps as the AlN layer is very thin. The longer thermally activated time transients observed after OFF-state trapping are associated with conventional traps at the surface on the gate–drain gap or inside the AlGaN barrier. These are accessible from the gate in the OFF state but not from the channel in the high-power state because of the relatively large electric field across the AlGaN barrier.

The defects at the AlGaN/AlN interface are perhaps intrinsic to the nature of this interface and the high stress under which AlN is grown. If our hypothesis is correct, this detrapping mechanism could be eliminated through the removal of AlN spacer layer.

Many studies have been devoted to buffer trapping which depends on the various types of traps that are introduced during the growth process [19]. Some buffer trapping could be present in the devices that are studied. Separation of buffer trapping, barrier trapping, and surface trapping is an important topic that is explored by other techniques [20]. The dynamic R_{ON} characterization methodology proposed in this paper should also be helpful to study this issue.

VI. Conclusion

In summary, we have developed a new methodology to investigate R_{ON} transients over arbitrary lengths of time. We have used this new technique to study trapping effects in high-voltage GaN HEMTs under a variety of pulsing conditions. In OFF-to-ON time transients, dynamic R_{ON} is enhanced up to several times of the original dc value, particularly as the OFF-state voltage increases. We have identified two distinct mechanisms with different timescales and temperature behavior. On a short timescale, the fast release of trapped charge takes place through a temperature-independent tunneling process. We postulate that interface states at the AlGaN barrier/AlN spacer interface are responsible for this. Conventional thermally assisted detrapping follows on a longer timescale. This postulate occurs from traps at the surface or inside the AlGaN barrier. In contrast, after a high power to ON switching, only fast detrapping through a temperature-independent process is observed. This is also consistent with trapping at the AlGaN/AlN interface. These findings provide a path to engineer a reliable GaN power-switching transistor with minimum dynamic R_{ON} problems.

Acknowledgment

The authors would like to thank Dr. J. Joh from Texas Instruments, Austin, TX, USA, for the helpful discussions.

References

[1] O. Ambacher, J. Smart, J. R. Shealy, N. G. Weimann, K. Chu, M. Murphy, W. J. Schaff, and L. F. Eastman, "Two-dimensional electron gases induced by spontaneous and piezoelectric polarization charges in N-and Ga-face AlGaN/GaN heterostructures," *J. Appl. Phys.*, vol. 85, no. 6, pp. 3222–3233, Mar. 1999.

[2] W. Saito, I. Omura, T. Ogura, and H. Ohashi, "Theoretical limit estimation of lateral wide band-gap semiconductor power-switching device," *Solid-State Electron.*, vol. 48, no. 9, pp. 1555–1562, Sep. 2004.

[3] S. C. Binari, P. B. Klein, and T. E. Kazior, "Trapping effects in GaN and SiC microwave FETs," *Proc. IEEE*, vol. 90, no. 6, pp. 1048–1058, Jun. 2002.

[4] G. Meneghesso, G. Verzellesi, F. Danesin, F. Rampazzo, F. Zanon, A. Tazzoli, M. Meneghini, and E. Zanoni, "Reliability of GaN high-electron-mobility transistor: State of the art and perspectives," *IEEE Trans. Device Mater. Rel.*, vol. 8, no. 2, pp. 332–343, Jun. 2008.

[5] G. Meneghesso, G. Verzellesi, R. Pierobon, F. Rampazzo, A. Chini, U. K. Mishra, C. Canali, and E. Zanoni, "Surface-related drain current dispersion effects in AlGaN-GaN HEMTs," *IEEE Trans. Electron Devices*, vol. 51, no. 10, pp. 1554–1561, Oct. 2004.

[6] R. Chu, A. Corrion, M. Chen, R. Li, D. Wong, D. Zehnder, B. Hughes, and K. Boutros, "1200-V normally off GaN-on-Si field-effect transistors with low dynamic on-resistance," *IEEE Electron Device Lett.*, vol. 32, no. 5, pp. 632–634, May 2011.

[7] M. Faqir, G. Verzellesi, A. Chini, F. Fantini, F. Danesin, G. Meneghesso, E. Zanoni, and C. Dua, "Mechanisms of RF current collapse in AlGaN–GaN high electron mobility transistors," *IEEE Trans. Device Mater. Rel.*, vol. 8, no. 2, pp. 240–247, Jun. 2008.

[8] B. Lu, T. Palacios, D. Risbud, S. Bahl, and D. Anderson, "Extraction of dynamic on-resistance in GaN transistors: Under soft-and hard-switching conditions," in *Proc. IEEE CSICS*, Oct. 2011, pp. 16–19.

[9] J. Joh and J. A. del Alamo, "A current-transient methodology for trap analysis for GaN high electron mobility transistors," *IEEE Trans. Electron Devices*, vol. 58, no. 1, pp. 132–140, Jan. 2011.

[10] D. Jin and J. A. del Alamo, "Mechanisms responsible for dynamic on-resistance in GaN high-voltage HEMTs," in *Proc. 24th ISPSD*, Jun. 2012, pp. 333–336.

[11] A. R. Arehart, A. Sasikumar, G. D. Via, B. Winningham, B. Poling, E. Heller, and S. A. Ringel, "Spatially-discriminating trap characterization methods for HEMTs and their application to RF-stressed AlGaN/GaN HEMTs," in *Proc. IEDM*, Dec. 2010, pp. 464–467.

[12] D. Jin and J. A. del Alamo, "Impact of high-power stress on dynamic ON-resistance of high-voltage GaN HEMTs," *Microelectron. Rel.*, vol. 52, no. 12, pp. 2875–2879, Dec. 2012.

[13] A. R. Arehart, A. Sasikumar, S. Rajan, G. D. Via, B. Poling, B. Winningham, E. R. Heller, D. Brown, Y. Pei, F. Recht, U. K. Mishra, and S. A. Ringel, "Direct observation of 0.57 eV trap-related RF output power reduction in AlGaN/GaN high electron mobility transistors," *Solid-State Elctron.*, vol. 80, pp. 19–22, Feb. 2013.

[14] N. Killat, M. Tapajna, M. Faqir, T. Palacios, and M. Kuball, "Evidence for impact ionization in AlGaN/GaN HEMTs with InGaN back-barrier," *Electron. Lett.*, vol. 47, no. 6, pp. 405–406, Mar. 2011.

[15] M. Meneghini, A. Stocco, R. Silvestri, G. Meneghesso, and E. Zanoni, "Degradation of AlGaN/GaN high electron mobility transistors related to hot electrons," *Appl. Phys. Lett.*, vol. 100, no. 23, pp. 233508-1–233508-3, Jun. 2012.

[16] S. A. Vitusevich,O. A. Antoniuk, M. V. Petrychuk, S. V. Danylyuk, A. M. Kurakin, A. E. Belyaev, and N. Klein, "Low-frequency noise in AlGaN/GaN HEMT structures with AlN thin film layer," *Phys. Status Solidi (C), Appl. Res.*, vol. 3, no. 6, pp. 2329–2332, May 2006.

[17] S. Huang, Q. Jiang, S. Yang, Z. Tang, and K. J. Chen, "Mechanism of PEALD-grown AlN passivation for AlGaN/GaN HEMTs: Compensation of interface traps by polarization charges," *IEEE Electron Device Lett.*, vol. 34, no. 2, pp. 193–195, Feb. 2013.

[18] D. M. Fleetwood, M. R. Shaneyfelt, and J. R. Schwank, "Estimating oxide-trap, interface-trap, and border-trap charge densities in metal-oxide-semiconductor transistors," *Appl. Phys. Lett.*, vol. 64, no. 15, pp. 1965–1967, Apr. 1994.

[19] M. J. Uren, J. Möreke, and M. Kuball, "Buffer design to minimize current collapse in GaN/AlGaN HFETs," *IEEE Trans. Electron Devices*, vol. 59, no. 12, pp. 3327–3333, Dec. 2012.

[20] D. W. Cardwell, A. R. Arehart, C. Poblenz, Y. Pei, J. S. Speck, U. K. Mishra, S. A. Ringel, and J. P. Pelz, "Nm-scale measurements of fast surface potential transients in an AlGaN/GaN high electron mobility transistor," *Appl. Phys. Lett.*, vol. 100, no. 19, pp. 193507-1–193507-4, May 2012.

Donghyun Jin (S'09) is currently pursuing the Ph.D. degree with the Massachusetts Institute of Technology, Cambridge, MA, USA.

He has been with Microsystems Technology Laboratories, Massachusetts Institute of Technology, since 2008.

Jesús A. del Alamo (S'79–M'85–SM'92–F'06) received the Ph.D. degree in electrical engineering from Stanford University, Stanford, CA, USA, in 1985.

He is currently a Donner Professor and MacVicar Faculty Fellow with the Massachusetts Institute of Technology, Cambridge, MA, USA.